International Food Research Journal 30(5): 1243 - 1260 (October 2023)
Journal homepage: *http://www.ifrj.upm.edu.my*

Concentration-dependent rheological characteristics of chickpea (*Cicer arietinum* L.) flour dispersion in steady and dynamic shear

[1]Das, R., [1]Kumar, Y., [1]Kaur, R., [2]Shekhar, S. and [1]*Prasad, K.

[1]*Department of Food Engineering and Technology, Sant Longowal Institute of Engineering and Technology, Longowal 148106, Punjab, India*
[2]*Department of Food Process Engineering, National Institute of Technology, Rourkela 769008, Odisha, India*

Article history

Received:
1 November 2022
Received in revised form:
16 March 2023
Accepted:
8 June 2023

Keywords

viscosity,
rheology,
viscoelasticity,
Cicer arietinum,
chickpea flour dispersion

Abstract

Chickpea (*Cicer arietinum* L.) flour (CF) is the basic raw material used in the form of dispersion in varied concentrations for making promising oriental sweets and snacks in the Asian subcontinent. The finished product quality of these fried food items thus mainly depends on the consistency of flour dispersions. Therefore, a concentration-dependent steady-state and dynamic rheological study, along with the pasting behaviour, was carried out. Steady shear rheology exhibited concentration-dependent pseudoplastic behaviour with significantly higher apparent viscosity for 40 - 45% CF dispersions, and a desirable consistency to be used in making fried sweets and snacks. The Herschel-Bulkley model described dispersions better at 5 - 20%, while Mizrahi-Berk at 25 - 50%. Hahn Ree-Erying's model described thixotropic behaviours for time-dependent flow; increasing CF concentration from 30 - 50% and increasing storage (G') and loss (G") modulus in the linear viscoelastic region. However, G' values were dominant over G" values in the small amplitude region, showing elastic behaviour, whereas viscous behaviour was exhibited in the higher amplitude region. During heating (30 - 80°C) in the temperature sweep test, concentrated samples (30 - 50%) showed a drastic increase in G' and complex viscosity (η*), while in cooling stages (95 - 25°C), a 25% concentration sample resulted in the highest values of G', G", and η*.

DOI
https://doi.org/10.47836/ifrj.30.5.13

Introduction

Chickpea (*Cicer arietinum* L.) is a vital legume crop that belongs to the family Fabaceae (Leguminosae) and sub-family Faboideae (Paplionaceae). It is the third most crucial legume crop after common beans (*Phaseolus vulgaris* L.) and peas (*Pisum sativum* L.) (Kumar *et al.*, 2018). Chickpea contributes about 24.34% to world pulse production, and India contributes around 69.76% to the total production during 2019 (FAO, 2021). Chickpea is highly popular as it is a cheaper source of proteins (20.9 - 25.27%), essential amino acids (methionine, cysteine, phenylalanine, tyrosine, and threonine), essential unsaturated fatty acids (linoleic acid, oleic acid, and linolenic acid), fibres (3%), carbohydrates (54 - 71%), vitamins (riboflavin, niacin, thiamine, and folate), and minerals (macro: Ca, Na, K, and Mg; micro: Zn, Fe, and Cu) (Rachwa-Rosiak *et al.*, 2015). It is directly consumed after soaking, germination, or roasting as these processes improve the digestibility, and eliminate the associated anti-nutritional factors (Kaur and Prasad, 2021b; 2022a; 2022b; 2023). Although chickpea is used as an edible seed, the seed coat is often removed during the dehulling process to produce chickpea split (*channa dhal*) and chickpea flour (CF, *besan*) (Prasad *et al.*, 2010). The suspension of dehulled flour in water is widely used for the preparation of various Indian traditional food products such as *boondi* (a spherical deep-fat fried product), *sev* (a cold extruded product followed by deep-fat frying), *dhokla* (steamed savoury cakes), and thin pancakes (*chilla*), both on a household as well as commercial scales.

*Corresponding author.
Email: profkprasad@gmail.com

Confectionary food items such as *Mysore pak*, *sohan papri* (prepared by CF with fat and sugar), and *laddu* (fried *boondi* deepened in sugar syrup and moulded into spherical-shaped balls) are also prepared from CF suspension (Kaur and Prasad, 2021a).

With modernisation in the production of traditional food products, knowledge of the rheological characteristics of CF suspensions provides instrumental quality control for raw materials before processing, intermediate products during manufacturing, and finished items after production. In addition, the rheological properties of flour suspensions in terms of shear stress and rate can provide essential information useful for many applications. It has been indicated that the rheological properties of dispersions depend on various factors, such as particle size, concentration, shear stress, time, and temperature. The discontinuous phase of soluble or insoluble particles is dispersed in a continuous phase (water), which is how they behave like shear thinning or thickening during the shear field.

Steady-state rheological parameters, such as flow behaviour and consistency index, diverge from Newtonian to non-Newtonian fluids, increasing suspension concentration and apparent viscosity. In addition, the estimation of yield stress is an important process parameter that determines the thickness of coating or spreading of flour suspensions on the surface of the food by pumping the liquid in a flow channel, thus preventing drip and slurry flow (Bhattacharya *et al.*, 2004). In practice, apparent viscosities of dispersions may depend not only on the shear rate but also on the time of shearing to which the slurry has been subjected. The significance of food's time-dependent rheological properties relates to the structural changes of material during the application of shear (the destruction of the internal structure during flow). During storage and transportation, the time-dependent rheological properties influence solid settling, phase separation, and stability of dispersions. Hence, it is imperative to understand the changes in the product during the process. Many of the foods that are thixotropic (showing a structural breakdown due to continuous application of shear) have been found similar in our study, such as rice-black gram suspensions, glutinous rice flour dispersions, and buckwheat starch-galactomannan mixtures (Bhattacharya and Bhat, 1997).

Consequently, the dynamic oscillatory properties have also been incorporated to characterise various slurry concentrations. For a clear understanding of elastic and viscous behaviour of samples, frequency, temperature, and amplitude sweep test are performed to obtain storage modulus (G'), loss modulus (G"), complex viscosity (η^*), and damping factor ($\tan\delta$ = G'/ G"). When measuring the viscoelastic properties of foods, the linear viscoelastic region is an important property where the applied stresses are inadequate to produce structural breakdown (yielding), and hence important microstructural properties can be measured at this point. Therefore, the linear viscoelastic region is determined experimentally by performing an amplitude sweep test, and thus this region corresponds to the point at which G' becomes stress or strain-dependent.

Several researchers have studied the effect of varying flour proportions on the rheological behaviour of sweet potato, basmati, and non-basmati rice flour. The rheological studies on CF are scarce and limited to the Spanish variety (flour to water concentrations of 1:5, 1:4, 1:3, and 1:2) and the Desi variety, cultivar A1 (concentration, w/w: 40%). However, all the reported studies have been performed at either lower concentrations or measured limited rheological properties, which might not be helpful during the formulation and preparation of coated food products. Higher concentrations (40 - 45%) may be required to prepare different fried food products such as *boondi*, *pakora*, and *bhujia*. Under the prevailing research gap, the present work was designed to study the effect of concentration (5 - 50%) on steady, dynamic, and temperature-dependent rheology, and their steady shear and time-dependent modelling of CF dispersions. The present work also examined the suitability of steady shear and time-dependent rheological models to predict the rheological parameters and the decay of shear stress with the time of shearing. The obtained findings may guide the selection criteria for appropriate concentrations of CF slurry for the commercial production of traditional Indian foods and other coated fried food items.

Materials and methods

Preparation of chickpea flour

The chickpea cultivar (PBG-7) was procured from Krishi Vigyan Kendra, Sangrur, Punjab. The grains were first cleaned and soaked in water at room temperature for 15 min to loosen the seed coat. The excess water was drained out, and the soaked grains were dried at 50°C in a tray dryer. The dried chickpea was dehulled to remove the seed coat, and split into cotyledons to form a chickpea split using a commercially available dehusker. The dehusked chickpea split was milled into flour using a hammer mill, and passed through a sieve of 100 mesh (150 µm). The obtained flour was then kept in airtight containers under refrigerated conditions (5°C) for further analysis.

Physico-chemical characterisation of dehusked chickpea flour

The proximate composition of the dehusked chickpea flour was determined following the standard method of AOAC (2002). The percentage of starch in flour was determined using the anthrone method (absorbance: 620 nm). The amylose content in flour was determined using the iodine method (590 nm). Loose bulk density (ρ_l), tapped bulk density (ρ_t), particle density (ρ_p), porosity (ε), Hausner's ratio, and Carr's index were calculated. The parameters Hausner's ratio and Carr's index are used for the determination of powder flowability. The static coefficient of friction was measured over different surface materials, namely plywood (parallel and perpendicular), galvanised iron sheet, and glass. Functional properties of the CF sample, such as water absorption capacity, were examined. Water solubility index and swelling power were determined at five different temperatures from 45 - 85°C at an interval of 10°C as per the procedure of Rafiq *et al.* (2015). All the tests were performed in triplicate.

Rheological characteristics

Preparation of various concentrations of CF dispersions

The lower concentration of chickpeas is often used to prepare beverages and soups. Therefore, it is important to control the quality to understand its flow behaviour (steady rheology) at different concentrations. In contrast, a higher slurry concentration is required to prepare coating and binding materials for conventional food products like fritters, *boondi*, and coated nuts. Therefore, dynamic rheology can provide a clear understanding of elastic and viscous behaviours.

For the prepared samples, chickpea flour (5 - 50%, w/v) was mixed manually with distilled water for 2 min to prepare the dispersions. Before rheological measurements, all prepared samples were kept enclosed to prevent moisture loss. Samples were gently blended for another 1 min before testing to ensure a uniform dispersion with no lumps. Steady and dynamic rheological measurements were performed using a rheometer (MCR 102, Anton Paar, Austria) with a parallel plate (50 mm diameter) and a measurement gap of 1 mm at 25°C.

Shear rate and time-dependent rheology

Shear stress and apparent viscosity of CF dispersion were measured between 5 and 100 s^{-1} to obtain 200 data points for all concentrations. For time-dependent rheology, each test was conducted for 5 min at a constant shear rate (5, 25, 50, and 100 s^{-1}) to obtain the data of shear stress (Pa) against the time of shearing (s).

Amplitude or strain sweep test and frequency sweep test

Oscillatory rheology was performed for concentrations higher than 30%, as lower concentrations are generally not preferred for coating and binding. An amplitude sweep test was performed to study flour dispersions' linear viscoelastic region. The storage modulus (G', Pa), loss modulus (G", Pa), and damping factor (tanδ) were measured between 0.01 and 100% of the applied strain at a constant angular frequency of 10 rad/s. The frequency sweep test was carried out between 0.1 and 100 rad/s at a constant strain of 0.5% based on the linear viscoelastic region. All the rheological tests were performed at 25°C unless otherwise specified.

Temperature sweep test

The lower concentration of chickpea flour in soups is cooked in water. In contrast, the high concentration slurry in coated and bound formulations is further cooked or fried to get the end products. The cooking of this formulation changed the viscoelastic behaviour with an increase in temperature. Therefore, to study the effect of temperature on the structural behaviour of CF dispersion, the samples were heated from 25 - 95°C at a rate of 5°C/min. The dynamic rheological parameters (G', G", and η*) were obtained as a function of temperature at a constant angular frequency (1 rad/s) and strain (0.5%).

Pasting properties

CF dispersion's pasting properties were analysed using a rapid visco analyser (Techmaster, Perten Instruments, Sweden) (Prasad *et al.*, 2013). Four different solid concentrations (5 - 20%) of slurry were prepared for the analysis of pasting properties. Higher concentration was not considered due to high viscosity, which resulted in a test failure. The dispersion was kept at 50°C for 1 min before being heated to 95°C in 3 min and 42 s. The cooked paste was held at 95°C for 2 min followed by cooling to 50°C in 3 min. At the start of the experiments, the paddle was rotated at 961 rpm, and after 12 s, the rotational speed of the paddle was maintained at a constant value of 160 rpm throughout the entire analysis. The rapid visco analyser profile was examined for the following responses: peak viscosity, holding strength, breakdown, total setback, final viscosity, and pasting temperature.

Theoretical considerations

Steady shear rheological models

Experimental data were fitted to the rheological models to describe the steady-state rheological characteristics. Power law, or the Oswald-de Waele model, is generally considered the most common and simple rheological model for describing the time-independent flow behaviour of inelastic fluid foods (Bhattacharya *et al.*, 1992). The model can be expressed as Eq. 1:

$$\sigma = K_P \gamma^{n_p} \quad \text{(Eq. 1)}$$

Casson, Herschel-Bulkley, and Mizrahi-Berk, or modified Casson models (Eq. 2, 3, and 4) were used to determine the yield stress term of the fluid foods:

$$\sigma^{0.5} = {\sigma_{0C}}^{0.5} + {\eta_C}^{0.5} \gamma^{0.5} \quad \text{(Eq. 2)}$$

$$\sigma = \sigma_{0HB} + K_{HB} \gamma^{n_{HB}} \quad \text{(Eq. 3)}$$

$$\sigma^{0.5} = \sigma_{0MB} + K_{MB} \gamma^{n_{MB}} \quad \text{(Eq. 4)}$$

where, K = consistency index, n = dimensionless flow behaviour index, η = plastic viscosity, and σ_0 = yield stress. From the Casson model, the parameters σ_{0C} and η_C were determined by drawing the straight line between the square root of shear stress ($\sigma^{0.5}$) and the square root of shear rate ($\gamma^{0.5}$) with the slope η_C and intercept σ_{0C}. The subscripts P, C, HB, and MB = Power law, Casson, Herschel-Bulkley, and Mizrahi-Berk models, respectively.

Time-dependent rheological models

The shear stress decay could be well described by three time-dependent rheological models widely used for describing the thixotropic (decrease in shear stress with time) and rheopectic (increase in shear stress with time) behaviours of foods. The model (Eq. 5) describes the logarithmic decay of stress without any equilibrium shear stress (Weltmann, 1943). The same model was modified by Hahn-Ree-Eyring to incorporate an equilibrium shear-stress value (Eq. 6). The stress decay process was described as a first-order kinetic model (Eq. 7) with a non-zero equilibrium term (Figoni and Shoemaker, 1981). Therefore, the relationship between shear stress σ(t) and time of shearing (t) can be given as:

$$\sigma(t) = A_1 - B_1 \, logt \quad \text{(Eq. 5)}$$

$$log[\sigma(t) - \sigma_e] = A_2 - B_2 t \quad \text{(Eq. 6)}$$

$$\sigma(t) = \sigma_e + (\sigma_0 - \sigma_e)\exp(-kt) \quad \text{(Eq. 7)}$$

where, the σ_e = equilibrium shear stress, σ_0 = initial shear stress, and k = stress decay during the time. A_1, B_1, A_2, and B_2 = rheological model parameters.

Coating application of chickpea slurry for making potato fritter

Potatoes of the Kufri Pukhraj variety were procured from the local farmhouse, Sangrur, Punjab. Quality potatoes with uniform size, shape, and colour were selected for experimentation. The washing of potatoes was carried out under running tap water to remove dirt and extraneous matter if adhered to the surface. Washed potatoes were peeled manually using a stainless-steel peeler. The peeled sample was put on a rectangular-shaped chipser and dicer (Platinum Chipser and Dicer, Millennium Products, Gujrat) to get potato fingers, and then they were trimmed to get uniform size for coating and frying experiments. The average size of each finger was maintained at 40 × 6.8 × 6.9 mm. The extent of coating of chickpea slurry of various concentrations (30 - 50%) on potato fingers and frying characteristics were studied. After coating, the samples were allowed to drip excess coating, then the dripping time and loss were noted. Atmospheric deep fat frying experiments were performed in an electrical fryer (VTL-5525, 230V-50Hz, 2000 W, Skyline, PRC) with a capacity of 5 L. The oil was preheated to the target temperature (160 ± 5°C) for 20 min, and maintained throughout the experiment. Then, the samples were fried to study the effect of chickpea slurry coating on the frying characteristics of developed fritter.

The moisture and oil contents of uncoated and coated fried potato fritters were determined using the standard method (AOAC, 2002). The surface colour was measured using a Hunter Lab colorimeter (Hunter Associates Laboratory Inc., Reston, VA, USA).

Statistical analysis

In order to elaborate on the variation in the rheological characteristics of CF dispersions under steady shear, statistical techniques were used to fit different rheological data (shear-stress/shear-rate and shear stress/time of shearing) to the well-known rheological models (time-independent: Power law, Casson, Herschel-Bulkley, and Mizrahi-Berk; time-dependent: Figoni and Shoemaker, Weltmann, and Hahn-Ree-Eyring) using non-linear regression analysis. The goodness of the models was judged by lower chi-square (χ^2), lower root mean square error (RMSE), and higher coefficient of multiple determination (R^2) values. Model fitting and data analysis for steady rheology were performed using the software OriginPro 2022 demo (OriginLab Corporation, Northampton, MA, USA.).

Results and discussion

Physicochemical and functional characterisation

The proximate compositions of dehusked chickpea flour (PBG-7), such as moisture, protein, fibre, fat, ash, and carbohydrate were determined, and are presented in Table 1. Similar results were obtained for the Desi chickpea variety (Ravi and Bhattacharya, 2004). The total starch, amylose, and amylopectin contents in CF were found to be 46.15, 20.67, and 25.48%, respectively. The physicochemical and functional characteristics of dehusked chickpea flour are shown in Table 1. The loose and tapped bulk densities were obtained as 380.99 ± 5.13 and 506.41 ± 9.07 kg/m^3, which correlated directly with Hausner's ratio and Carr's index values. Lower loose bulk density increased Hausner's ratio and Carr's index values. The powder particles' density can be related to the moisture content, structure, and size of the particles. In the present work, the values of Hausner's ratio and Carr's index ranged between 1.35 - 1.45 and 26 - 31%, respectively, thus resulting in poor flowability properties. It is mainly due to the lower particle size (≤ 150 μm) which provides more compact points for inter-particle attraction. However, the fine particles provide a higher Van der Walls force due to the larger contact surface areas of individual particles. Higher particle size of the flour results in better flowability, whereas reduction in particle size leads to increased cohesiveness, thus hindering the flowability of flour. This is because of the increased contact points, which increase interparticle bonding (Fitzpatrick *et al.*, 2004). Therefore, the particle size of the flour is an important parameter that affects the flow behaviour. These results correlated with the findings of skim milk powder (particle size < 150 μm; Hausner's ratio = 1.40 ± 0.03; Carr's index = 28.50 ± 1.73%) (Pugliese *et al.*, 2017). The particle size of the flour also affected the bulk and tapped densities, which in turn were correlated with the flowability of the flour. The coarse particles had lower compaction properties as compared to fine powders that settled rapidly after tapping (Abdullah and Geldart, 1999).

The static coefficient of friction on four different surfaces showed the highest values for plywood (corrugated perpendicular line surface) than other surfaces. This surface required a higher gravitational force to overcome the frictional forces between the flour and horizontal base, thereby resulting in a greater ϕ value. In comparison to glass, very little force is acting on the material to fall down due to the smoother surface.

The water absorption capacity was found to be 1.62 ± 0.13 g/g, which describes the ability of flour to absorb water and swell in order to enhance the food consistency. Water absorption capacity also affects the ability of CF to form a paste, and is important in food systems to improve yield and give body to the food systems. On the other hand, the water solubility index and swelling power increased from 6.7 ± 0.19 - 16.5 ± 0.14% and 2.79 ± 0.11 - 8.78 ± 0.03 with an increase in temperature (45 - 85°C). When the dispersion is heated above gelatinisation temperature, the crystalline structure of starch granules is broken down and water molecules become linked with the exposed ─OH group of amylose and amylopectin through hydrogen bonding, causing starch molecules to swell and increase in solubility (Rafiq *et al.*, 2015). The highest water solubility index and swelling power for CF were obtained at 85°C, where most of the granules were gelatinised. Therefore, it is important to characterise the sample before doing the

Table 1. Physicochemical characteristics of dehusked chickpea flour.

Parameter		
Proximate composition		
Moisture content (% db)		9.45 ± 0.15
Protein content (% db, N × 6.25)		22.77 ± 0.25
Crude fibre (% db)		2.63 ± 0.20
Fat (% db)		4.20 ± 0.10
Ash (% db)		2.46 ± 0.02
Carbohydrate (% db, by difference method)		58.49 ± 0.04
Starch (% db)		46.15 ± 0.56
Amylose (% db)		20.67 ± 0.21
Amylopectin (% db)		25.48 ± 0.58
Gravimetric property		
Loose bulk density (ρ_l, kg/m^3)		389.49 ± 1.23
Tapped bulk density (ρ_t, kg/m^3)		563.50 ± 11.21
Particle/solid density (ρ_t, kg/m^3)		1257.0 ± 11.19
Porosity ($1 - \rho_l/\rho_p$)		69.29 ± 0.39
Powder flowability property		
Hausner's ratio ($HR = \rho_t/\rho_l$)		1.45 ± 0.03
Carr's index (%, $CI = \frac{\rho t - \rho l}{\rho t} \times 100$)		29.89 ± 0.22
Frictional property		
Static coefficient of friction		
Glass		0.28 ± 0.02
Plywood (P_1: corrugated parallel line surface)		0.36 ± 0.03
Galvanized iron sheet		0.42 ± 0.04
Plywood (P_1: corrugated perpendicular line surface)		0.46 ± 0.02
Angle of repose (°, $\phi = \tan^{-1}\frac{2H}{b}$)		38.70 ± 1.15
Functional property		
Water absorption capacity (g/g, $WAC = W_{sd}/W_s$)		1.62 ± 0.13
Water solubility index (%, $WSI = W_{ds}/W_s \times 100$)		
	45°C	6.70 ± 0.19
	55°C	8.70 ± 1.27
	65°C	11.80 ± 1.13
	75°C	14.30 ± 0.71
	85°C	16.50 ± 0.14
Swelling power ($SP = \frac{W_{ws} \times 100}{W_s \times (100 - \%WSI)}$)		
	45°C	2.79 ± 0.11
	55°C	3.71 ± 0.84
	65°C	4.78 ± 0.02
	75°C	7.41 ± 0.14
	85°C	8.78 ± 0.03

W_{ds} = weight of dry solid in supernatant; W_s = initial weight of sample; W_{sd} = weight of water in sediment; and W_{ws} = weight of wet sediment. Values are mean value ± S.D.

rheological experiments. Since the physicochemical and functional properties affect the rheological characteristics of dehusked CF, they can be used to relate the rheological properties. Water solubility is also linked with the presence of amylose, sugars, albumins, and other water-soluble fractions. The fine particles generally show high solubility in water (Ahmed *et al.*, 2014). On the other hand, the swelling index is representative of the ability of starch molecules to absorb water at a specific temperature.

The composition of starch, that is, amount of amylose and amylopectin, is the major factor affecting the pasting behaviour of flour. Particle size also affects the pasting viscosity of the flour. The presence of fine particles result in high viscosity. The presence of high amount of protein content negatively affects the swelling of starch molecules as it restricts the water to reach starch globules that are imbedded in protein matrix (Bolade *et al.*, 2009; Bala *et al.*, 2020).

Rheological characteristics

Steady shear rheology

The shear stress (σ) and viscosity versus shear rate for different concentrations of dehusked CF dispersions (5 - 50%) at 25°C are presented (Figures 1A and 1B).

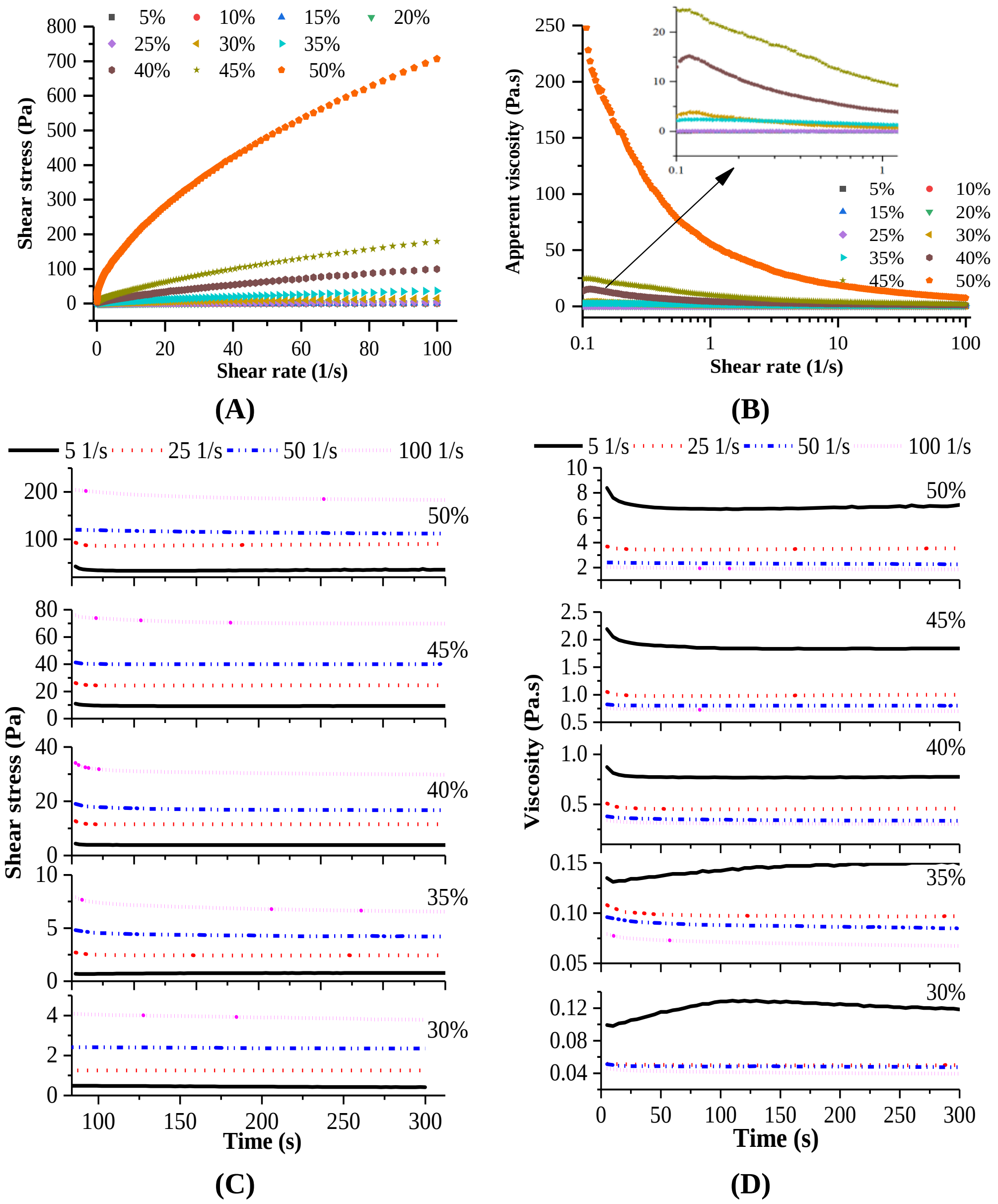

Figure 1. Steady rheology of CF flour suspensions at 25°C. **(A)** and **(B)**: shear stress (σ) and apparent viscosity (η) plot as a function of shear rate (γ); **(C)** and **(D)**: change in shear stress and apparent viscosity with time at a constant shear rate (5, 25, 50, and 100 1/s).

The increase in batter concentration and shear rate increased the shear stress, and the pattern of the curve suggested non-Newtonian pseudoplastic behaviour having concentration-dependent specific yield stress. The yield stress (σ_e) is the minimum shear stress at which the material will deform or start to flow without a significant load increase. It is related to the internal molecular structure and binding properties of materials that must be deformed to initiate any flow. For chickpea slurry, the yield stress is significant in preparing coated food products like fritters (batter-coated fried potatoes, coated fried panner, *etc*.). The yield stress values of various flour dispersions are determined using three well-known steady-shear rheological models: Casson, Herschel-Bulkley, and Mizrahi-Berk. It was observed that an increase in dispersion concentration increased the yield stress, consistency index (K), and plastic viscosity (η). This was mainly due to increased rigidity and strength, and an improvement in the supramolecular network structure.

The power-law model parameters could well describe the flow behaviour of CF slurry as presented in Table 2. All the flour dispersions had shown shear-thinning flow behaviour with a lower flow index (n_P < 1). The shear-thinning nature might have been due to the breakdown of entangled polysaccharides' molecular network during shearing. In addition, as the shear rate increased, the disruption rate of intermolecular entanglements became higher than the reformation rate because of the hydrodynamic forces generated during shearing. Consequently, the disruption rate caused a reduction in the fluid resistance of the sample matrix, and resulted in a decreased apparent viscosity (η). Similar kinds of findings were also observed for rice flour dispersions (Ma *et al.*, 2020) and buckwheat starch-galactomannan mixtures (Choi and Chang, 2012). Those concentration-dependent parameters (η and K) may find useful applications for setting guidelines for predicting the rheological characteristics of formulated foods containing CF.

The consistency (K) and flow behaviour index (n) for different concentrations of CF dispersions (5 - 50%) varied from 0.009 - 51.456 and 0.659 - 0.569 (Power law model), -0.006 - 5.48 and 0.880 - 0.6 (Herschel-Bulkley model), and 0.0047 - 10.751 and 0.027 - 5.456 - 0.556 - 0.329 (Mizrahi-Berk model), respectively (Table 3). All the models were able to fit the flow behaviour with R^2 > 0.922. However, the Herschel-Bulkley model showed high goodness of fit for the concentrations of 5 - 20% ($0.968 \leq R^2 \leq 0.998$; $0.009 \leq$ RMSE ≤ 0.015; and $7.2 \times 10^{-5} \leq \chi^2 \leq 2.1 \times 10^{-4}$), whereas the Mizrahi-Berk model was suitable for the higher concentrations of slurry ranging from 25 - 50% ($R^2 = 0.999$; $0.019 \leq$ RMSE ≤ 0.228; and $3.7 \times 10^{-4} \leq \chi^2 \leq 0.052$).

Time-dependent rheology

The time-dependent rheology of CF dispersion at different concentrations and shear rates are shown in Figures 1C and 1D. When the shear rate was increased, shear stress decreased in the initial 100 s, and can be explained as thixotropic behaviour. However, once initial resistance was overcome, shear stress approached a constant value between 100 and 300 s. The observed time-dependent flow behaviour of dehusked CF slurry was modelled using three suitable rheological models: Figoni and Shoemaker, Weltmann, and Hahn-Ree-Eyring models, and their model parameters with R^2, RMSE, and χ^2 values are shown in Table 3. These time-dependent models are well known to describe the thixotropy behaviour of food (Ibarz and Barbosa-Cánovas, 2003). The parameters A_1 and A_2 (Eqs. 5 and 6, respectively) represent the shear stress (Pa) required for the structure to start degrading, whereas parameters B_1 and B_2 indicate the quality and speed of structural degradation during shearing. Nevertheless, the parameters B_2 and k are related to the stress decay with shearing. The values of the Weltman model parameters (A_1 and B_1) increased with an increase in shear rate and concentration, and were unable to fit well at the higher concentrations (40 - 50%) with low shear rates. However, none of these three models was able to fit well for the 50% concentration at shear rates of 5 and 25 s^{-1}. This was mainly due to higher concentration with the application of low shear conditions, thus resulting in higher shear stress with respect to time, known as the rheopectic behaviour of slurry.

HRE model parameters (A_2 and B_2) varied unevenly with shear rates. Based on the parameter values obtained from the three models, the HRE model was better fitted for all the concentrations except 35% (shear rate: 5 s^{-1}) and 50% concentration, whereas the Weltman model was better fitted for 35% concentration at a shear rate of 5 s^{-1}.

Table 2. Suitability of steady shear rheological models and parameters with R^2, RMSE, and χ^2 values for various concentrations (5 - 50%) of CF sample. Values are mean ± S.D.

Concentration (%)	Model and model parameter			R^2	RMSE	χ^2
	Power law $\sigma = K_P\gamma^{n_P}$					
	K_P	**n_P**				
5	0.009 ± 5.7 × 10^{-4}	0.659 ± 0.016		0.948	0.011	1.2 × 10^{-4}
10	0.01 ± 2.5 × 10^{-4}	0.776 ± 0.006		0.995	0.006	4.0 × 10^{-5}
15	0.015 ± 3.1 × 10^{-4}	0.805 ± 0.005		0.997	0.008	6.9 × 10^{-5}
20	0.034 ± 6.1 × 10^{-4}	0.775 ± 0.004		0.997	0.015	2.3 × 10^{-4}
25	0.089 ± 8.2 × 10^{-4}	0.82 ± 0.002		0.999	0.023	5.2 × 10^{-4}
30	0.617 ± 0.011	0.67 ± 0.005		0.996	0.215	0.046
35	1.184 ± 0.009	0.744 ± 0.002		0.999	0.212	0.045
40	3.965 ± 0.028	0.703 ± 0.002		0.999	0.591	0.349
45	8.491 ± 0.058	0.664 ± 0.002		0.999	1.116	1.245
50	51.456 ± 0.337	0.569 ± 0.002		0.999	5.321	28.311
	Casson $\sigma^{0.5} = \sigma_{0C}{}^{0.5} + \eta_C{}^{0.5}\gamma^{0.5}$					
	σ_{0C}	**η_C**				
5	0.0092 ± 8.5 × 10^{-6}	0.001 ± 5.5 × 10^{-7}		0.922	0.026	7.0 × 10^{-4}
10	0.004 ± 3.5 × 10^{-6}	0.003 ± 2.3 × 10^{-7}		0.986	0.056	2.9 × 10^{-4}
15	0.007 ± 1.5 × 10^{-6}	0.005 ± 1.1 × 10^{-7}		0.996	0.012	1.4 × 10^{-4}
20	0.008 ± 9.9 × 10^{-6}	0.011 ± 6.7 × 10^{-7}		0.988	0.030	9.0 × 10^{-4}
25	0.008 ± 2.4 × 10^{-5}	0.04 ± 1.6 × 10^{-6}		0.992	0.046	0.002
30	0.365 ± 1.8 × 10^{-5}	0.105 ± 1.25 × 10^{-6}		0.998	0.041	0.002
35	0.313 ± 1.6 × 10^{-4}	0.34 ± 1.09 × 10^{-6}		0.994	0.121	0.015
40	1.405 ± 4 × 10^{-4}	0.899 ± 2.7 × 10^{-6}		0.994	0.192	0.037
45	3.401 ± 0.001	1.575 ± 8.1 × 10^{-4}		0.990	0.330	0.109
50	26.479 ± 0.008	5.664 ± 0.005		0.982	0.834	0.696
	Herschel-Bulkley $\sigma = \sigma_{0HB} + K_{HB}\gamma^{n_{HB}}$					
	σ_{0HB}	**K_{HB}**	**n_{HB}**			
5	-0.006 ± 9.9 × 10^{-4}	0.003 ± 3.7 × 10^{-4}	0.880 ± 0.025	0.968	0.009	7.2 × 10^{-5}
10	-0.001 ± 7.1 × 10^{-4}	0.008 ± 3.1 × 10^{-4}	0.816 ± 0.009	0.996	0.017	3.3 × 10^{-5}
15	0.004 ± 6.9 × 10^{-4}	0.011 ± 2.7 × 10^{-4}	0.862 ± 0.006	0.998	0.006	3.4 × 10^{-5}
20	0.006 ± 0.002	0.031 ± 8.6 × 10^{-4}	0.791 ± 0.006	0.998	0.015	2.1 × 10^{-4}
25	0.006 ± 0.003	0.096 ± 0.001	0.805 ± 0.003	0.999	0.020	4.1 × 10^{-4}
30	0.306 ± 6.9 × 10^{-4}	0.419 ± 0.004	0.753 ± 0.002	0.999	0.053	0.003
35	0.215 ± 0.027	1.141 ± 0.014	0.752 ± 0.003	0.999	0.205	0.042
40	1.22 ± 0.069	3.673 ± 0.038	0.719 ± 0.002	0.999	0.495	0.245
45	2.16 ± 0.117	7.67 ± 0.07	0.686 ± 0.002	0.999	0.806	0.650
50	5.48 ± 0.504	44.5 ± 0.358	0.6 ± 0.002	0.999	2.993	8.955
	Mizrahi-Berk $\sigma^{0.5} = \sigma_{0MB} + K_{MB}\gamma^{n_{MB}}$					
	σ_{0MB}	**K_{MB}**	**n_{MB}**			
5	0.103 ± 0.005	0.027 ± 0.004	0.556 ± 0.032	0.923	0.026	7 × 10^{-4}
10	0.026 ± 0.005	0.087 ± 0.004	0.406 ± 0.010	0.991	0.014	2.1 × 10^{-4}
15	0.060 ± 0.003	0.086 ± 0.002	0.460 ± 0.005	0.997	0.010	1.1 × 10^{-4}
20	-4.5 × 10^{-4} ± 0.005	0.193 ± 0.005	0.375 ± 0.005	0.997	0.016	2.7 × 10^{-4}
25	-0.062 ± 0.006	0.335 ± 0.006	0.392 ± 0.003	0.999	0.019	3.7 × 10^{-4}
30	0.497 ± 0.005	0.427 ± 0.004	0.440 ± 0.002	0.999	0.019	3.6 × 10^{-4}
35	0.187 ± 0.012	0.946 ± 0.011	0.397 ± 0.002	0.999	0.039	0.002
40	0.611 ± 0.019	1.506 ± 0.017	0.402 ± 0.002	0.999	0.063	0.004
45	0.719 ± 0.025	2.36 ± 0.024	0.368 ± 0.002	0.999	0.074	0.006
50	2.029 ± 0.094	5.456 ± 0.092	0.329 ± 0.003	0.999	0.228	0.052

Table 3. Time dependent rheological model (Figoni and Shoemaker, Weltmann, and Hahn-Ree-Eyring) parameters with R^2, RMSE, and χ^2 values for various concentrations of CF sample (30 - 50%) as a function of shear rates (5, 25, 50, and 100 s^{-1} at 25°C). Values are mean ± S.D.

Concentration (%)	Shear rate (s^{-1})	Model and model parameter			R^2	RMSE	χ^2
		Figoni and Shoemaker $\sigma(t) = \sigma_e + (\sigma_0 - \sigma_e)\exp(-kt)$					
		σ_e [Pa]	**σ_0 [Pa]**	**k [s^{-1}]**			
30	5	0.405	0.500	$0.006 \pm 2.1 \times 10^{-4}$	0.864	0.011	1.2×10^{-4}
	25	1.250	1.280	0.040 ± 0.003	0.814	0.003	8.2×10^{-6}
	50	2.350	2.474	0.005 ± 0.001	0.954	0.007	5.4×10^{-5}
	100	3.790	4.580	$0.009 \pm 4.5 \times 10^{-4}$	0.978	0.026	6.6×10^{-4}
35	5	0.753	0.673	$0.012 \pm 3.9 \times 10^{-4}$	0.934	0.007	4.9×10^{-5}
	25	2.430	2.690	0.074 ± 0.003	0.954	0.009	7.4×10^{-5}
	50	4.220	4.800	$0.018 \pm 4.1 \times 10^{-4}$	0.945	0.028	7.7×10^{-4}
	100	6.540	7.910	$0.013 \pm 2.7 \times 10^{-4}$	0.940	0.072	0.005
40	5	3.840	4.360	0.122 ± 0.005	0.911	0.018	3.1×10^{-4}
	25	11.50	12.70	0.147 ± 0.008	0.852	0.052	0.017
	50	16.70	19.00	$0.024 \pm 6.0 \times 10^{-4}$	0.942	0.105	0.011
	100	30.01	33.06	0.018 ± 0.001	0.934	0.194	0.038
45	5	9.210	11.00	0.078 ± 0.003	0.915	0.065	0.004
	25	24.50	26.20	0.143 ± 0.011	0.748	0.105	0.748
	50	40.00	41.20	0.110 ± 0.004	0.921	0.040	0.002
	100	69.80	76.00	$0.018 \pm 2.0 \times 10^{-4}$	0.990	0.144	0.020
50	5	35.60	42.60	Not fitted			
	25	90.30	92.70	Not fitted			
	50	112.0	120.1	$0.009 \pm 1.5 \times 10^{-4}$	0.971	0.402	0.162
	100	182.3	204.1	$0.012 \pm 5.4 \times 10^{-5}$	0.998	0.234	0.055
		Weltmann $\sigma(t) = A_1 - B_1 \log t$					
		A_1 [Pa]	**B_1 [Pa.s^{-1}]**				
30	5	0.59 ± 0.002	0.069 ± 0.001		0.820	0.012	1.6×10^{-4}
	25	$1.27 \pm 5.3 \times 10^{-4}$	$0.013 \pm 2.5 \times 10^{-4}$		0.715	0.003	9.6×10^{-6}
	50	2.55 ± 0.002	$0.082 \pm 7.3 \times 10^{-4}$		0.926	0.009	8.0×10^{-5}
	100	3.42 ± 0.003	0.422 ± 0.003		0.963	0.032	0.001
35	5	$0.596 \pm 7 \times 10^{-4}$	$-0.067 \pm 3.2 \times 10^{-4}$		0.976	0.004	1.6×10^{-5}
	25	2.59 ± 0.004	0.074 ± 0.002		0.670	0.022	4.7×10^{-4}
	50	4.946 ± 0.003	0.302 ± 0.002		0.975	0.019	3.4×10^{-4}
	100	8.382 ± 0.008	0.73 ± 0.004		0.970	0.049	0.002
40	5	Not fitted					
	25	Not fitted					
	50	19.222 ± 0.036	1.065 ± 0.017		0.975	0.069	0.005
	100	34.351 ± 0.048	1.843 ± 0.0223		0.985	0.091	0.008
45	5	Poorly fitted					
	25	Not fitted					
	50	Not fitted					
	100	78.145 ± 0.038	3.532 ± 0.018		0.975	0.220	0.048
50	5	Not fitted					
	25	Not fitted					
	50	126.46 ± 0.35	5.69 ± 0.170		0.919	0.682	0.687
	100	216.04 ± 0.43	13.427 ± 0.207		0.977	0.829	0.048

Hahn-Ree-Eyring (HRE) $log[\sigma(t) - \sigma_e] = A_2 - B_2 t$								
		σ_e [Pa]	A_2 [Pa]	B_2 [Pa.s^{-1}]				
30	5	0.405	-2.203 ± 0.023	0.007 ± 2.84 × 10^{-4}	0.897	0.012	1.6 × 10^{-4}
	25	1.250	-3.154 ± 0.005	0.058 ± 0.004	0.880	0.002	5.8 × 10^{-6}
	50	2.350	-2.076 ± 0.021	0.009 ± 2.8 × 10^{-4}	0.954	0.007	5.4 × 10^{-5}
	100	3.790	-0.419 ± 0.005	0.009 ± 4.5 × 10^{-4}	0.978	0.026	6.6 × 10^{-4}
35	5		Not fitted				
	25	2.430	-1.167 ± 0.031	0.079 ± 0.003	0.965	0.007	0.008
	50	4.220	-0.705 ± 0.019	0.015 ± 4.1 × 10^{-4}	0.970	0.021	4.5 × 10^{-4}
	100	6.540	0.132 ± 0.013	0.011 ± 2.1 × 10^{-4}	0.980	0.042	0.002
40	5	3.840	0.145 ± 0.210	0.30 ± 0.055	0.981	0.008	6.8 × 10^{-5}
	25	11.50	1.005 ± 0.033	0.275 ± 0.008	0.983	0.018	0.017
	50	16.70	0.635 ± 0.021	0.019 ± 5.5 × 10^{-4}	0.969	0.077	0.006
	100	30.01	1.115 ± 0.031	0.018 ± 7.7 × 10^{-4}	0.934	0.194	0.037
45	5	9.210	0.756 ± 0.045	0.094 ± 0.005	0.924	0.067	0.004
	25	24.50	1.289 ± 0.098	0.252 ± 0.023	0.854	0.080	0.006
	50	40.00	0.642 ± 0.031	0.167 ± 0.006	0.974	0.023	5.4 × 10^{-4}
	100	69.80	1.757 ± 0.010	0.017 ± 2.2 × 10^{-4}	0.993	0.116	0.014
50	5	35.60	Not fitted				
	25	90.30	Not fitted				
	50	112.0	2.181 ± 0.013	0.010 ± 1.9 × 10^{-4}	0.980	0.335	0.113
	100	183.0	3.071 ± 0.004	0.013 ± 6.8 × 10^{-5}	0.999	0.204	0.042

Dynamic rheology

Foods are complex materials that exhibit both liquid and solid-like properties, and are categorised as viscoelastic materials. The elastic modulus (G') measures the deformation energy stored by the sample which reflects the solid characteristics. In contrast, the viscous modulus (G") is a measure of dissipated or lost energy per oscillation to indicate the liquid property (Okonkwo *et al.*, 2021). The complex viscosity (η*) signifies the overall viscosity of the system. The mechanical spectra of five different concentrations (30, 35, 40, 45, and 50%) of CF slurry are displayed in Figure 2. It was observed that at lower strain (0.01 - 1%), G' and G" for all the dispersions increased with concentration but exhibited linear viscoelastic behaviour. However, once strain was increased over 1%, G' and G" increased slightly, followed by a continuous decrease till 100% strain once structure failed. The linear viscoelastic region indicates the material's ability to maintain its original structure (unbroken) under applied strain (Kowalski *et al.*, 2017). The decrease in G' and G" at higher amplitude regions can be related to the breakdown of starch and protein molecules, which caused a reduction in the molecular size of the samples. Hence, the strength of a supramolecular network was decreased in the samples, which further decreased the solid/rigid/elastic behaviour and G'. A similar trend was followed for oat flours (Li *et al.*, 2021). In contrast, the damping or loss factor (tanδ = G"/G') for all the samples was less than or greater than 1, thus showing the viscoelastic behaviour of fluid in Figure 2A. A damping factor less than 1 indicates predominately elastic behaviour, whereas a damping factor greater than 1 indicates predominately viscous behaviour (Singh and Kaur, 2017). In the present work, the G' value was higher than G" value when the concentration of CF dispersions ranged from 30 - 40% with the applied strain up to 2.51%, and showed elastic behaviour (tanδ < 1). However, when the applied strain was more than 2.51%, a viscous behaviour of dispersion was observed as the material yield or fractures (Razavi *et al.*, 2018). In addition, at 45 and 50% concentrations, due to the dense structure, elastic behaviour was observed up to 6.31% strain, which was almost double in comparison to 30 - 40% samples. Hence, from these observations, it can be concluded that higher strain was required for higher concentration dispersions to show completely viscoelastic behaviour.

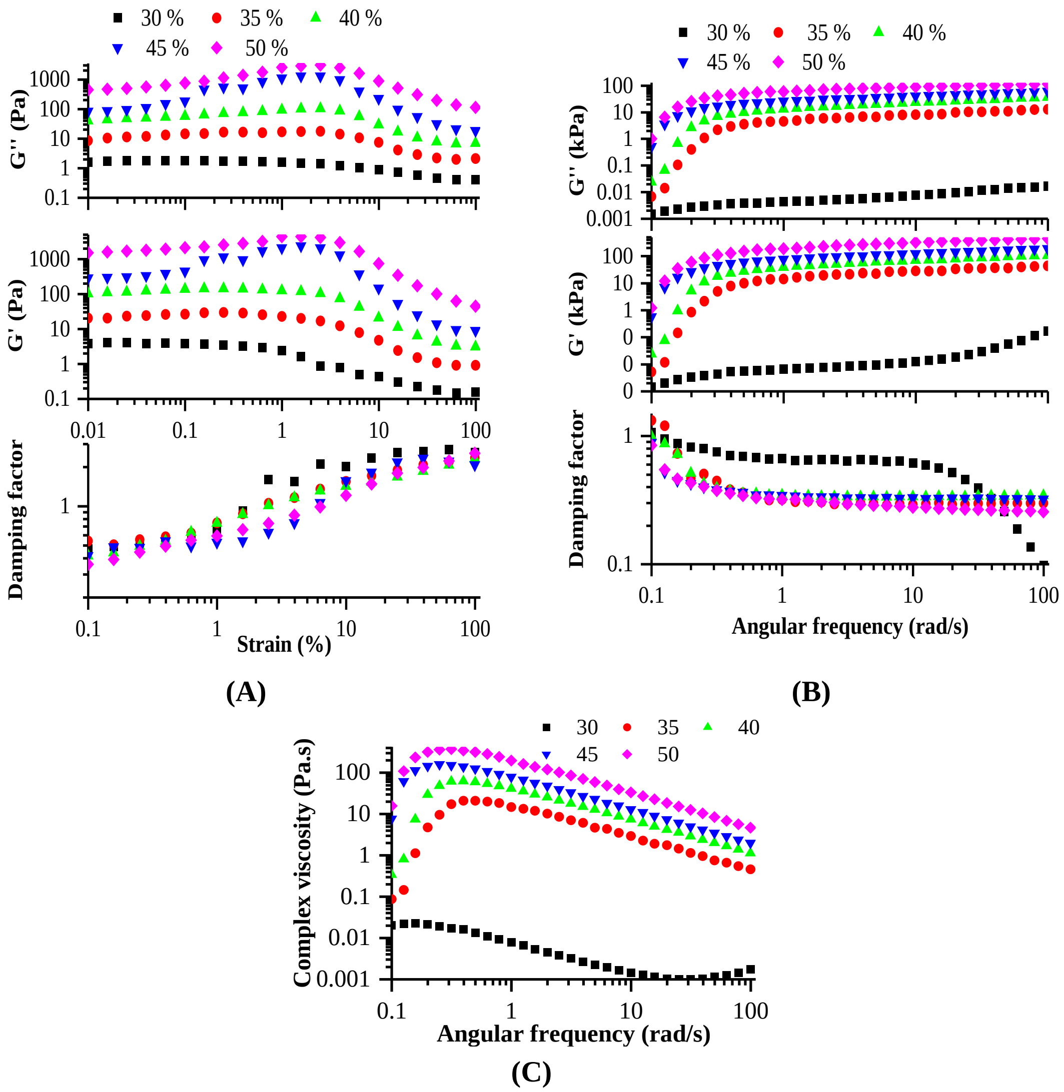

Figure 2. Dynamic rheology of CF suspensions. **(A)**: AST at 25°C, strain = 0.01 - 100%, ω = 10 rad/s; **(B)**: FST = 25°C, strain = 0.5%, ω = 0.1-100 rad/s; and **(C)**: complex viscosity.

The frequency sweep test performed in linear viscoelastic region at 0.5% strain (Figure 2B) showed that the magnitudes of G' and G" increased with an increase in ω and flour concentration. In addition, the complex viscosity (a measure of overall flow resistance) decreased with the increase in ω (Figure 2C) for all the dispersions, and showed a shear-thinning flow behaviour in accordance with the previously described steady-state rheological study. The G' values were found to be higher than the G" values over the angular frequency ranges of 0.1 - 100 rad/s, showing that there are quite fast molecular movements and no specific intermolecular interaction (Palavecino *et al.*, 2020). This could be due to the fact that the oscillation time of reassociation of the chain is longer than that of disentanglement, thus resulting in solid/elastic properties dominating viscous behaviour (Ahmed *et al.*, 2007). The frequency-dependent G' and G" in batters or slurries can be expressed as evidence of the presence of a supramolecular network structure. It also indicates a rigid network presence in the batter, which may be due to the breakdown of larger molecular structure compounds and the increase in the number of binding sites in dispersions. As a result, a rigid supramolecular structure was formed, enhancing the batter's elastic/solid characteristics rather than its viscous properties (Das and Bhattacharya, 2019). A similar kind of observation was reported elsewhere for fluid and semi-solid foods, oat bran protein flour, and Indian coffee plum pulp. Due to the increase in G' over G" at all the frequency values, the damping or loss factor (tanδ = G"/ G') was found to be less than 1, which showed the similar behaviour of CF slurry (Figure 2B).

Temperature sweep test

The effect of temperature on the viscoelastic properties of batter was investigated to better understand the structural changes caused by temperature variations encountered during processing and storage (Rao, 2010). The temperature dependency of G', G", and η* is shown in Figure 3. It was observed that G' values for all the samples were dominant over G" values, thus indicating that all the samples showed more elastic than viscous behaviour during heating (tanδ < 1). At lower concentrations (5 - 25%), G' and η* were almost constant during heating from 25 - 70°C, thus revealing no major structural changes. However, at increased concentrations (30 - 50%), a drastic increase in G', and η* was observed when the sample was heated from 30 - 80°C. However, the same trend was followed for lower concentrations as heating continued (70 - 80°C). The increase in G' can be accounted for by the swelling of starch granules that encountered each other, thereby occupying a larger fraction of the dispersions, providing higher rigidity to the system. In contrast, a drastic increase in G" values for all the samples was observed during heating from 30 - 80°C. The increase in G" with increased temperature was mainly due to the leaching of amylose molecules from swollen starch granules to form a continuous network that showed viscous behaviour (Singh and Kaur, 2017). However, with further heating (80 - 95°C) of all the samples, no G', G", and η* changes were observed.

During cooling (95 - 25°C), the G', G", and η* values increased. However, at the start of the cooling phase, the G', G", and η* values for the lower concentration sample increased drastically, while these results for the higher concentrations did not change much. This was due to the fact that lower concentration samples were quickly retrograded as compared to higher concentration samples. At the cooling stages, it was observed that the G', G", and η* values for the intermediate concentration sample (25%) had shown a maximum peak. This might have been due to the presence of a higher amount of gelatinised starch as compared to other concentrations, which have undergone retrogradation (Wu *et al.*, 2016).

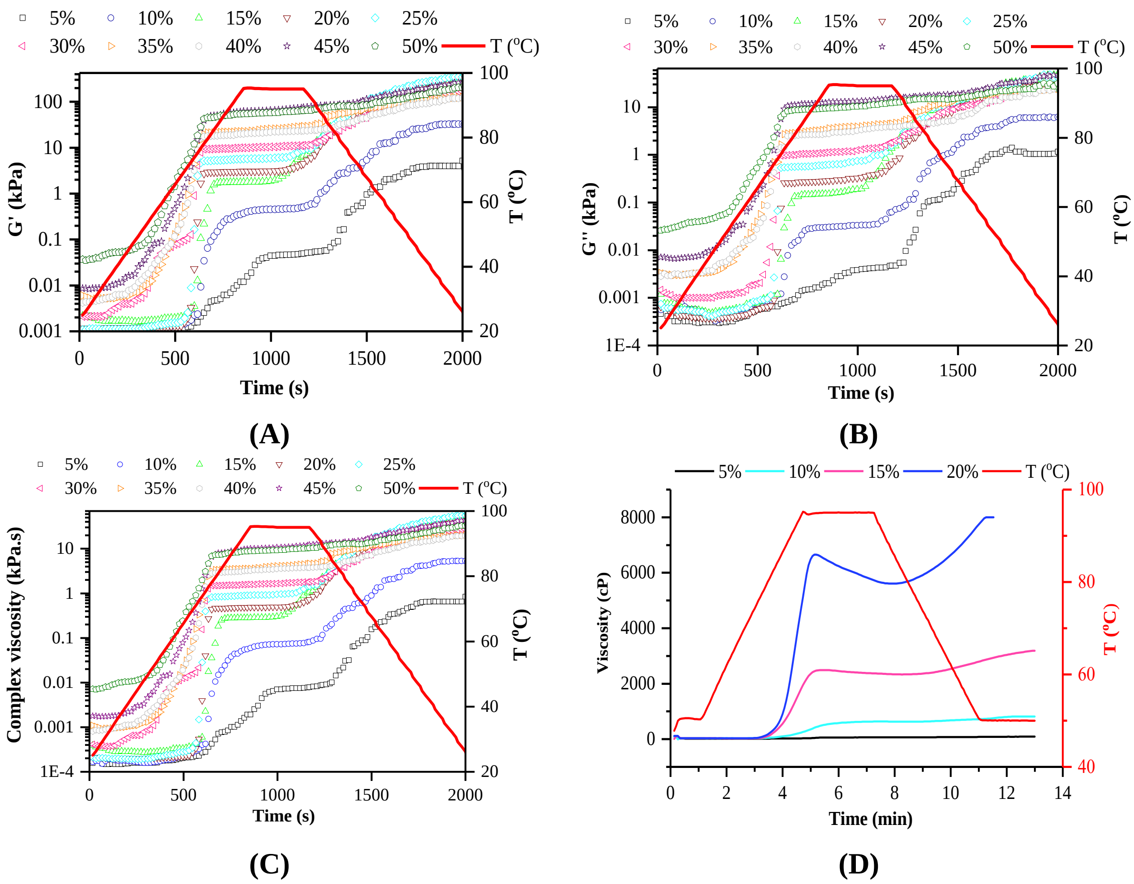

Figure 3. Effect of temperature on **(A)**: storage modulus (G'); **(B)**: loss modulus (G"); and **(C)**: complex viscosity (η*) of various concentration of CF suspensions (5, 10, 15, 20, 25, 30, 35, 40, 45, and 50%), and **(D)**: RVA curve. The viscoelastic properties were measured under controlled conditions (TST = 25 - 95 and 95 - 25°C, ω = 1 rad/s, strain = 0.5%).

Pasting properties

In general, the pasting properties are based on the gelatinisation temperature of starch. It was observed that the increase in flour concentrations increased the viscosity parameters such as peak viscosity, holding strength, breakdown, final viscosity, total setback, and peak temperature from 58 - 6652 cP, 54 - 5607 cP, 4 - 1045 cP, 82 - 8000 cP, 28 - 2383 cP, and 73.5 - 78.25°C, respectively (Figure 3D). During heating, all the dispersions showed a gradual increase in viscosity. This may be attributed to the removal of water from the extended amylose molecules as they swell (Ghiasi *et al.*, 1982; Kheto *et al.*, 2022). A similar profile is reported for CF (Spanish chickpea variety) slurries containing flour-to-water ratios of 1:5, 1:4, 1:3, and 1:2. They found that increasing concentrations did not show any peak viscosity during the heating ramp, but during the holding phase, viscosity progressively increased. The peak viscosity was reported at 87°C for the highest concentration (1:2) of slurry. However, in the present work, the pasting temperature was reported higher for higher concentrations, thus indicating the presence of starch, which is highly resistant to swelling and rupturing.

Similarly, breakdown is a parameter that shows intense knowledge about the magnitude of the drop in viscosity during heating. It is instrumental in determining the degree of starch solubility during heating and shearing in a starch water system (Prasad *et al.*, 2013). The lowest setback viscosity was observed at a lower flour concentration (5%), thus indicating a lower tendency to retrograde. The capacity to lower retrogradation is advantageous in a variety of culinary products, such as soups and sauces, whereas retrogradation causes higher viscosity (Prasad and Singh, 2014). During cooling at 50°C, an increase in viscosity was observed for all the samples, which revealed that the paste could convert into a gel.

Effect of chickpea batter coating on the quality of potato fritters

Chickpea flour slurry of various concentrations was used as the coating material of potato finger as the inner material in the present work. Generally, a coating material is used to protect the base or inner material from the exposure of intense heat, and also to avoid any ill effect on the flavour and nutritional characteristics during deep-fat frying. Slurry, coating material, or the batter consistency has a major influence on the amount of coating picked by the base material, and decides the frying time, oil content, and colour of the fried product. The amount of batter picked up by the sample during coating was significantly ($p < 0.05$) higher at a higher batter concentration (50%), as shown in Table 4. It was illustrated that the way the coating picked up depended on the rheological properties of the batter. The higher batter concentration contained a higher solid content and protein to starch ratio, which increased their ability to bind water and increased viscosity (Dogan *et al.*, 2005), and simultaneously improved the nutritional characteristics. As a result, the higher batter concentration created stronger adhesive forces (mechanical forces: sticking together; and electrostatic forces: attraction due to opposing charges) with the wetting surface of the slab, causing slurry to cling and spread over the slab. These findings correlated with the previously reported article for an increase in viscosity and adhesion with increasing protein to starch ratio in the batter (Kılınççeker and Kurt, 2010).

Dripping time (s) is the time required to drip the batter droplets after coating until they stop, which was found to be maximum at higher concentrations. After coating, the drip loss (g/100 g) was increased with concentration to a maximum of 45%, followed by a decrease to 50%. The possible reason for decreasing drip loss at 50% concentration could have been due to a thick and viscous coating adhering tightly to the surface of the potato slab.

The moisture content, oil content, and colour properties of uncoated and coated potato fritters at optimised conditions were evaluated, and are presented in Table 4. It was evident that the frying time increased with increasing batter concentrations, mainly due to the formation of a thicker coating at higher concentrations, which delayed the heat penetration to the core of the slab. The moisture content of fried products was comparable and found in the range of 60.22 - 62.96%. However, the oil content of the fried products varied significantly ($p < 0.05$) from 8.56% for control to 26.64% for 35%. It was observed that the product oil content increased with batter concentration from 0 - 35%, followed by a gradual decrease when the batter concentration ranged from 40 - 50%. Gradual decrease in oil after

Table 4. Properties of uncoated and coated fried potato fingers.

	0	30	35	40	45	50
	Coating material of chickpea flour at various concentration (%)					
Potato fritter before frying						
Coating wt (g/100 g potato)	-	13.85 ± 1.65[a]	21.18 ± 1.64[b]	27.27 ± 1.77[c]	44.83 ± 1.88[d]	80.97 ± 2.77[e]
Dripping time (s)	-	15.00 ± 2.00[a]	19.33 ± 3.21[b]	34.75 ± 7.76[c]	56.67 ± 7.57[d]	85.33 ± 12.90[e]
Drip loss (g/100 g potato)	-	8.74 ± 1.71[a]	23.39 ± 3.09[b]	55.66 ± 4.92[c]	74.23 ± 2.04[e]	64.31 ± 5.25[d]
	Properties of fried potato finger					
Fried potato						
Frying time (s)	180	180	240	330	390	420
Moisture content (%)	60.41 ± 1.25[a]	62.72 ± 0.99[b]	60.22 ± 0.45[a]	60.22 ± 1.11[a]	62.96 ± 0.47[b]	62.08 ± 0.57[b]
Oil content (%)	8.56 ± 0.16[a]	15.67 ± 0.22[c]	26.64 ± 0.34[f]	19.18 ± 0.15[e]	17.73 ± 0.34[d]	12.75 ± 0.55[b]
Lightness (L*)	65.75 ± 0.96[c]	57.50 ± 3.87[b]	56.75 ± 3.59[ab]	59.00 ± 3.37[b]	53.25 ± 2.22[a]	55.25 ± 4.11[a]
Redness (a*)	7.25 ± 0.96[a]	12.00 ± 3.74[b]	11.75 ± 1.50[b]	16.50 ± 2.65[c]	11.50 ± 1.29[b]	12.25 ± 0.96[b]
Yellowness (b*)	45.75 ± 2.06[a]	47.75 ± 0.96[a]	47.00 ± 3.83[a]	47.75 ± 2.87[a]	44.25 ± 1.71[a]	46.75 ± 4.65[a]

Lowercase superscripts in the same row indicate significant effect ($p < 0.05$) on the properties of uncoated and coated fried potato slab.

40 - 50% concentrations was observed due to efficient barrier properties at higher concentrations, which significantly reduced the oil penetration to the potato slab. Minor variations in the lightness, redness, and yellowness values of fried fritters were observed due to the frying time selected, thus ensuring that all samples were properly cooked without overcooking.

Conclusion

The physicochemical properties of dehusked CF (PBG-7 variety) affected the rheological properties of flour dispersions. All the pasting parameters such as peak viscosity, holding strength, break down, final viscosity, total setback, and peak temperature were increased from 58 - 6652 cP, 54 - 5607 cP, 4 - 1045 cP, 82 - 8000 cP, 28 - 2383 cP, and 73.5 - 78.25°C, respectively, with an increase in flour concentrations (5 - 20%). In steady-state shear rheological measurements, an increase in batter concentration and shear rate increased the shear stress. The curve pattern suggested non-Newtonian pseudoplastic behaviour having concentration-dependent specific yield stress. However, the Herschel-Bulkley model showed high goodness of fit for the concentrations of 5 - 20% ($0.968 \leq R^2 \leq 0.998$; $0.009 \leq$ RMSE ≤ 0.015; and $7.2 \times 10^{-5} \leq \chi^2 \leq 2.1 \times 10^{-4}$). In contrast, the Mizrahi-Berk model was suitable for the higher concentration of slurry ranging from 25 - 50% ($R^2 = 0.999$; $0.019 \leq$ RMSE ≤ 0.228; and $3.7 \times 10^{-4} \leq \chi^2 \leq 0.052$). HRE model well explained the thixotropic behaviour of slurry with $R^2 \geq 0.854$, RMSE ≤ 0.335, and $\chi^2 \leq 0.113$. It was thus concluded that depending on the concentration-dependent pseudoplastic behaviour, viscosity for 40 - 45% CF dispersions with desirable consistency could be used in making fried sweets and snacks. The amplitude sweep test determined a linear viscoelastic region with strain up to 1%. During the frequency sweep test and amplitude sweep test, the G' value was dominant over the G" value, thus indicating pseudoplastic and more elastic than viscous behaviour. During the temperature sweep test, G' and η* values for the lower concentration (5 - 25%) samples were almost unchanged. In contrast, in the cooling phase, maximum peaks (G', G", and η*) were observed at intermediate concentrations (25%), thus indicating maximum retrogradation. The observed data may be potentially helpful for designing the equipment and guiding the selection criteria for appropriate concentrations of CF slurry for the commercial production of Indian traditional foods and other coated fried foods.

Acknowledgement

The authors would like to express cordial thanks to Director, Sant Longowal Institute of Engineering and Technology, Longowal, India for extending the support to complete this work. Further, authors express their gratitude to the All-India Council for Technical Education (AICTE), New Delhi, India for providing necessary support as AICTE Doctoral Fellowship (ADF).

References

Abdullah, E. C. and Geldart, D. 1999. The use of bulk density measurements as flowability indicators. Powder Technology 102(2): 151-165.

Ahmed, J., Al-Foudari, M., Al-Salman, F. and Almusallam, A. S. 2014. Effect of particle size and temperature on rheological, thermal, and structural properties of pumpkin flour dispersion. Journal of Food Engineering 124: 43-53.

Ahmed, J., Ramaswamy, H. S. and Sashidhar, K. C. 2007. Rheological characteristics of tamarind (*Tamarindus indica* L.) juice concentrates. LWT - Food Science and Technology 40(2): 225-231.

Association of Official Analytical Chemists (AOAC). 2002. Official methods of analysis of AOAC International - Standard methods for the examination. United States: AOAC.

Bala, M., Handa, S., Mridula, D. and Singh, R. K. 2020. Physicochemical, functional and rheological properties of grass pea (*Lathyrus sativus* L.) flour as influenced by particle size. Heliyon 6(11): e05471.

Bhattacharya, S. and Bhat, K. K. 1997. Steady shear rheology of rice-blackgram suspensions and suitability of rheological models. Journal of Food Engineering 32(3): 241-250.

Bhattacharya, S., Bhat, K. K. and Raghuveer, K. G. 1992. Rheology of Bengal gram (*Cicer arietinum*) flour suspensions. Journal of Food Engineering 17(2): 83-96.

Bhattacharya, S., Latha, R. B. and Bhat, K. K. 2004.

Controlled stress rheological measurement of blackgram flour dispersions. Journal of Food Engineering 63(2): 135-139.

Bolade, M. K., Adeyemi, I. A. and Ogunsua, A. O. 2009. Influence of particle size fractions on the physicochemical properties of maize flour and textural characteristics of a maize-based nonfermented food gel. International Journal of Food Science and Technology 44(3): 646-655.

Choi, D. W. and Chang, Y. H. 2012. Steady and dynamic shear rheological properties of buckwheat starch-galactomannan mixtures. Preventive Nutrition and Food Science 17(3): 192.

Das, A. B. and Bhattacharya, S. 2019. Characterization of the batter and gluten-free cake from extruded red rice flour. LWT - Food Science and Technology 102: 197-204.

Dogan, S. F., Sahin, S. and Sumnu, G. 2005. Effects of soy and rice flour addition on batter rheology and quality of deep-fat fried chicken nuggets. Journal of Food Engineering 71(1): 127-132.

Figoni, P. I. and Shoemaker, C. F. 1981. Characterization of structure breakdown of foods from their flow properties. Journal of Texture Studies 12(3): 287-305.

Fitzpatrick, J. J., Barringer, S. A. and Iqbal, T. 2004. Flow property measurement of food powders and sensitivity of Jenike's hopper design methodology to the measured values. Journal of Food Engineering 61(3): 399-405.

Food and Agriculture Organization (FAO). 2021. FAOSTAT - Food and agriculture data. United States: FAO.

Ghiasi, K., Varriano-Marston, E. and Hoseney, R. C. 1982. Gelatinization of wheat starch. II. Starch-surfactant interaction. Cereal Chemistry 59(2): 86-88.

Ibarz, A. and Barbosa-Cánovas, G. V. 2003. Food preservation by cooling - Unit operations in food engineering. 1st ed. United States: CRC Press.

Kaur, R. and Prasad, K. 2021a. Nutritional characteristics and value-added products of chickpea (*Cicer arietinum*) - A review. Journal of Postharvest Technology 9(2): 1-13.

Kaur, R. and Prasad, K. 2021b. Technological, processing and nutritional aspects of chickpea (*Cicer arietinum*) - A review. Trends in Food Science and Technology 109: 448-463.

Kaur, R. and Prasad, K. 2022a. Effect of malting and roasting of chickpea on functional and nutritional qualities of its protein fractions. International Journal of Food Science and Technology 57(7): 3990-4000.

Kaur, R. and Prasad, K. 2022b. Elucidation of chickpea hydration, effect of soaking temperature, and extent of germination on characteristics of malted flour. Journal of Food Science 87(5): 2197-2210.

Kaur, R. and Prasad, K. 2023. Elucidation of temperature dependent hydration behaviour of chickpea seeds: Prerequisite for germination. Biocatalysis and Agricultural Biotechnology 50: 102669.

Kheto, A., Das, R., Deb, S., Bist, Y., Kumar, Y., Tarafdar, A. and Saxena, D. C. 2022. Advances in isolation, characterization, modification, and application of *Chenopodium* starch: A comprehensive review. International Journal of Biological Macromolecules 222: 636-651.

Kılınççeker, O. and Kurt, Ş. 2010. Effects of chickpea (*Cicer arietinum*) flour on quality of deep-fat fried chicken nuggets. Journal of Food, Agriculture and Environment 8(2): 47-50.

Kowalski, R. J., Meldrum, A., Wang, S., Joyner, H. and Ganjyal, G. M. 2017. Waxy wheat flour as a freeze-thaw stable ingredient through rheological studies. Food and Bioprocess Technology 10(7): 1281-1296.

Kumar, M. M., Prasad, K., Sarat Chandra, T. and Debnath, S. 2018. Evaluation of physical properties and hydration kinetics of red lentil (*Lens culinaris*) at different processed levels and soaking temperatures. Journal of the Saudi Society of Agricultural Sciences 17(3): 330-338.

Li, Y., Obadi, M., Shi, J., Xu, B. and Shi, Y.-C. 2021. Rheological and thermal properties of oat flours and starch affected by oat lipids. Journal of Cereal Science 102: 103337.

Ma, M., Wen, Y., Qiu, C., Zhan, Q., Sui, Z. and Corke, H. 2020. Milling affects rheological and gel textural properties of rice flour. Cereal Chemistry 97(2): 205-215.

Okonkwo, V. C., Mba, O. I., Kwofie, E. M. and Ngadi, M. O. 2021. Rheological properties of meat sauces as influenced by temperature. Food and Bioprocess Technology 14(11): 2146-2160.

Palavecino, P. M., Penci, M. C. and Ribotta, P. D. 2020. Effect of sustainable chemical modifications on pasting and gel properties of sorghum and cassava starch. Food and Bioprocess Technology 13(1): 112-120.

Prasad, K. and Singh, Y. 2014. Rice based vegetable supplemented functional instant soup mix: Development and optimization. Germany: Scholars' Press.

Prasad, K., Anil, A., Singh, Y. and Sinha, A. S. K. 2013. Concentration dependent rheological behaviour of promising basmati and non basmati rice flour. International Food Research Journal 20(4): 2005-2008.

Prasad, K., Vairagar, P. R. and Bera, M. B. 2010. Temperature dependent hydration kinetics of *Cicer arietinum* splits. Food Research International 43(2): 483-488.

Pugliese, A., Cabassi, G., Chiavaro, E., Paciulli, M., Carini, E. and Mucchetti, G. 2017. Physical characterization of whole and skim dried milk powders. Journal of Food Science and Technology 54(11): 3433-3442.

Rachwa-Rosiak, D., Nebesny, E. and Budryn, G. 2015. Chickpeas—Composition, nutritional value, health benefits, application to bread and snacks: A review. Critical Reviews in Food Science and Nutrition 55(8): 1137-1145.

Rafiq, S. I., Jan, K., Singh, S. and Saxena, D. C. 2015. Physicochemical, pasting, rheological, thermal and morphological properties of horse chestnut starch. Journal of Food Science and Technology 52(9): 5651-5660.

Rao, M. A. 2010. Rheology of fluid and semisolid foods: Principles and applications. United States: Springer Science and Business Media.

Ravi, R. and Bhattacharya, S. 2004. Flow behaviour of chickpea (*Cicer arietinum* L.) flour dispersions: Effect of additives. Journal of Food Engineering 65(4): 619-624.

Razavi, S. M. A., Alghooneh, A. and Behrouzian, F. 2018. Influence of temperature on sage seed gum (*Salvia macrosiphon*) rheology in dilute and concentrated regimes. Journal of Dispersion Science and Technology 39(7): 982-995.

Singh, S. and Kaur, M. 2017. Steady and dynamic shear rheology of starches from different oat cultivars in relation to their physicochemical and structural properties. International Journal of Food Properties 20(12): 3282-3294.

Weltmann, R. N. 1943. Breakdown of thixotropic structure as function of time. Journal of Applied Physics 14(7): 343-350.

Wu, K., Gan, R., Dai, S., Cai, Y. Z., Corke, H. and Zhu, F. 2016. Buckwheat and millet affect thermal, rheological, and gelling properties of wheat flour. Journal of Food Science 81(3): E627-E636.